*Kinetics and Catalysis, Vol. 45, No. 4, 2004, pp. 467–477. Translated from Kinetika i Kataliz, Vol. 45, No. 4, 2004, pp. 498–508.*


# Mechanism of the Formation of Molybdenum Metallocarbene Complexes in the Gas Phase

**V. B. Goncharov**

*Boreskov Institute of Catalysis, Siberian Division, Russian Academy of Sciences, Novosibirsk, 630090 Russia*

Received November 28, 2002

**Abstract**—The reactions of $Mo^+$ ions and $Mo_xO_y^+$ oxygen-containing molybdenum cluster ions ($x$ = 1–3; $y$ = 1–9) with methane, ethylene oxide, and cyclopropane were studied using ion cyclotron resonance. The formation of a number of organometallic ions, including the metallocarbene $MoCH_2^+$, as well as molybdenum oxometallocarbenes $Mo_xO_yCH_2^+$ ($x$ = 1–3; $y$ = 2, 4, 5, or 8) and $Mo_xO_y(CH_4)^+$ ions ($x$ = 1–3; $y$ = 2, 5, or 8), was detected. The upper and lower limits of bond energies in oxometallocarbene complexes were evaluated: $111 > D^0(Mo_xO_y^+–CH_2) > 82$ kcal/mol ($x$ = 1–3; $y$ = 2, 5, 8).

## INTRODUCTION

The disproportionation reaction of olefins (metathesis) was discovered in 1964 [1]. This reaction provides an opportunity to perform selective conversion of alkenes into other alkenes (with higher or lower molecular weights). Because of this, practical applications of this conversion in petroleum chemistry are of interest. The above reaction consists of the exchange of carbene fragments between olefin molecules.

The ions of metals (Mo, W, and Re) catalyze this reaction [1–3]. It is well known that the metathesis of olefins is a rapid reversible process with complex kinetics; the order of the reaction with respect to olefin depends on the olefin/catalyst ratio. Initially, it was believed that the exchange of carbene fragments included the simultaneous coordination of both olefin molecules followed by the cleavage of C=C bonds and the formation of new bonds. However, it was found that this is a chain process, and the carbene mechanism [2–4] (Scheme 1) is commonly accepted. The first step of this mechanism is the formation of intermediate **I**, in which the alkyldiene moiety of an olefin forms a double bond with the metal ion (see Scheme 1).

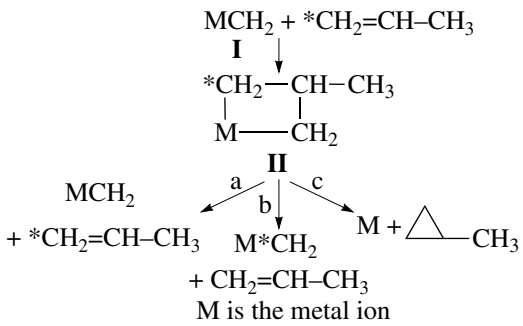


**Scheme 1.**

Next, the olefin molecule is coordinated to metallocarbene intermediate **I**. In this case, the formation of a four-centered intermediate metal–cyclopropane complex **II** is postulated, which can undergo decomposition via a few reaction paths: (a) the reaction of degenerated metathesis (i.e., the carbon skeleton of the olefin remains unchanged in this case), (b) the metathesis reaction, and (c) the formation of cyclopropane derivatives (chain termination).

Thus, the generation step of intermediate **I** is the key step in the carbene mechanism of olefin metathesis reactions. Catalysts of various types generate metallocarbenes by different mechanisms.

Several conceivable reaction paths for the formation of such intermediates were considered in the literature [3]. Olefin metathesis catalysts can be tentatively subdivided into the following three groups: (1) catalysts that require the presence of organometallic cocatalysts (usually alkyl metals), (2) catalysts containing carbene groups, and (3) catalysts directly activated by olefins.

It is well known that, in systems of the first type, the cocatalyst reduces the ions of a catalytically active metal. In this case, organometallic compounds of the catalytically active metal with bound alkyl groups are formed. The conversion of a bound alkyl into a coordinated carbene ligand results from the direct elimination of a hydrogen atom from the alkyl carbon atom at the α-position.

Systems of the second type consist of individual compounds containing carbene groups, for example, $(CO)_5W=C(Ph)_2$, or they form carbene groups directly in the course of reaction, for example, in the decomposition of diazo compounds in the presence of tungsten compounds [5].

Systems of the third type are heterogeneous catalysts; these are mainly Group VI metal (Mo and W)

0023-1584/04/4504-0467 © 2004 MAIK "Nauka/Interperiodica"

oxides, as well as Re and Ta oxides. These systems can be active in the absence of cocatalysts. In systems of this type, a metal–carbene complex should result from the interaction of an olefin with the transition metal ion of the catalyst. Either olefin isomerization by hydride transfer or the reaction of two coordinated olefin molecules with the formation and subsequent isomerization of a metallocycle are usually considered as possible mechanisms of this interaction.

It is well known that $MoO_3$ and $WO_3$ can be reduced by carbon monoxide or hydrogen; they can also be photoreduced. Thereafter, the catalytic activity of the above oxides toward the reaction of olefin metathesis dramatically increased [4]. This fact is related to the formation of reduced metal ions (in oxidation states of +4 and +5) and to the presence of free coordination sites at these ions.

In recent years, a great number of publications have been devoted to the reactions of isolated metal atoms in hydrocarbon matrices at reduced temperatures and to the reactions of metal ions with hydrocarbons in the gas phase. The behavior of Group VIII cations was primarily studied. The composition of products suggests that the reaction occurs via addition at C–H and/or C–C bonds followed by the conversion of organometallic intermediates. These studies are of great interest for understanding the chemical nature of the elementary acts in the heterogeneous catalytic conversions of hydrocarbons, and they can serve as an experimental basis for describing reaction mechanisms. The gas-phase studies of the reactivity of small cluster metal oxo ions can be currently performed using mass-spectrometric techniques, such as tandem mass spectrometry (or an ion-beam technique), ion cyclotron resonance (ICR) spectrometry, etc. [6, 7]. Gas-phase reactions can be considered as the simplest models of the interaction of the active centers of oxide catalysts with substrate molecules. The reactions of the cluster oxo ions of molybdenum are of particular interest because they can model the interaction of molecules with the surface fragments of oxide catalysts. The reactions of molybdenum ions in the gas phase were practically not studied because the main seven isotopes of molybdenum produce very complicated mass spectra, especially in the case of cluster ions. Previously [8, 9], attention was focused on the preparation and fragmentation of the cluster oxo ions of molybdenum in the gas phase.

In this work, an effort is made to prepare a set of the cluster oxo ions of molybdenum $Mo_xO_y^+$ ($x$ = 1–3; $y$ = 1–9) and to study their reactions with methane and cyclopropane (cyclo-$C_3H_6$). The reaction with cyclo-$C_3H_6$ on solid molybdenum trioxide or prereduced (chemically (with CO or $H_2$) or photochemically) supported molybdenum trioxide resulted in the formation of the metallocarbene oxo complexes of molybdenum. This reaction is frequently used for the initiation of olefin metathesis. The study of the interaction of the oxo ions of molybdenum containing various numbers of oxygen and molybdenum atoms provides an opportunity to examine the effects of factors like coordination unsaturation and oxidation state on the reactivity of the metal center. The effect of ligands (oxygen atoms) on the composition of the resulting intermediates was also under examination.

## EXPERIMENTAL

The experiments were performed on a Bruker Spectrospin CMS-47 ICR mass spectrometer with an Oxford Instruments vertical-field cryomagnet (4.7 T), which was equipped with a cubic cell (33 mm) for ion trapping [10]. The vacuum system of the spectrometer was pumped out to a base pressure of $(1–2) \times 10^{-9}$ mbar using an ion pump with a pumping speed of 160 l/s; the plates of the ion trapping cell were maintained at room temperature. An ionization gage was used for pressure measurements. Neutral clusters of molybdenum oxo ions were generated by the evaporation of molybdenum trioxide from a quartz Knudsen cell, which was equipped with a bifilar heater and mounted on the retaining plate of the ICR cell on the anode side. This design provided the heating of the cell over the temperature range 300–900 K without considerable gas evolution and magnetic field destabilization. The temperature was controlled with the use of a Chromel–Alumel thermocouple based on a temperature–heater current calibration curve ($\alpha$-$Al_2O_3$ powder was used as a standard substance). The ratio between surface areas was $S/s > 1500$, where $S$ is the internal surface area of the Knudsen cell, and $s$ is the surface area of the opening. Molybdenum trioxide (V/O Izotop) with an enrichment of 97% in the $^{98}$Mo isotope was used. The use of a monoisotopic sample (the natural abundance of molybdenum isotopes is as follows (%): $^{92}$Mo 61.5, $^{94}$Mo 38.3, $^{95}$Mo 65.9, $^{96}$Mo 39.6, $^{98}$Mo 100.0; and $^{100}$Mo 39.9) made it possible to simplify the mass spectra and to improve the sensitivity of the technique to heavy ions by one order of magnitude.

The oxo ions of molybdenum were prepared by the electron-impact ionization (70 eV) of molybdenum trioxide vapor. The pressure of methane or cyclopropane in the vacuum system was usually equal to $\sim(1–2) \times 10^{-7}$ mbar. The ICR spectrum was excited using a standard pulse sequence and repeated several tens of times in order to obtain an acceptable signal-to-noise ratio. The ICR spectra were measured in the Fourier transform mode. The mass window was varied from 2 to 10 amu depending on the test mass range. The ratios between ionic products were measured with an accuracy of 10%.

A double resonance technique was used for studying the mechanisms of ion–molecule reactions in the gas phase. This technique provides an opportunity for removal of parent ions with a given mass-to-charge ratio at the beginning of each experiment. In this case, changes observed in the ICR spectrum provide information on the reactions.

Figure 1 demonstrates the mass spectrum of the oxo ions of molybdenum (70 eV) obtained by the evaporation of $^{98}MoO_3$ at 600 K. Figure 1 indicates that cluster oxo ions of molybdenum $Mo_xO_y^+$ containing various numbers of metal and oxygen atoms were formed. All the concomitant ions were removed at the beginning of each experiment with the use of the double resonance technique. The remaining ions with a chosen *m*/*z* reacted with neutral molecules, then the reaction products were detected.

The kinetic method of the destructive addition of ligands was used for the experimental determination of metal–ligand bond energies. Let us consider the reaction of a metal ion $M^+$ with a neutral molecule $L_1L_2$

$$M^+ + L_1L_2 \longrightarrow ML_1^+ + L_2. \qquad \text{(I)}$$

Because the ICR technique makes it possible to observe only exothermic reactions, the formation of $ML_1^+$ ions indicates that the lower limit of the ion bond strength ($D^0(M^+–L_1)$) is greater than the bond strength in the neutral molecule ($D^0(L_1–L_2)$). However, the absence of the products of reaction (I) can not always be considered as evidence for the fact that the upper limit of the $M^+–L_1$ bond strength is lower than $D^0(L_1–L_2)$ because a great energy barrier may exist.

The binding energy of oxygen atoms in the cluster oxo ions of molybdenum was estimated with the use of the following thermodynamic cycle:

$$\begin{array}{ccc} M^+ - L & \xrightarrow{D^0(ML^+)} & M^+ + L \\ \uparrow IP(ML^+) & & \uparrow IP(M^+) \\ M - L & \xrightarrow{D^0(ML)} & M + L \end{array} \qquad \text{(II)}$$

$$D^0(M^+–L) = D^0(M–L) + IP(M) – IP(ML).$$

Table 1 summarizes the calculated values of $D^0(M^+–L)$ together with the binding energies of oxygen in neutral molecules and the ionization potentials (*PI*s) taken from [11]. Data given in Table 1 indicate that the cluster oxo ions of molybdenum with $MoO_3$ stoichiometry exhibited the weakest bond with oxygen. Thus, the maximum reactivity of these ions, that is, $(MoO_3)_x^+$, in reactions with methane and cyclopropane would be expected.

The structures of various molybdenum oxo ions were studied with the use of a simple model of paired potentials [12]. The molecular geometry parameters were obtained by minimizing total molecular energies with the use of the following potential function:

$$U_t = U_{MO} + U_{MM} + U_{OO}. \qquad (1)$$

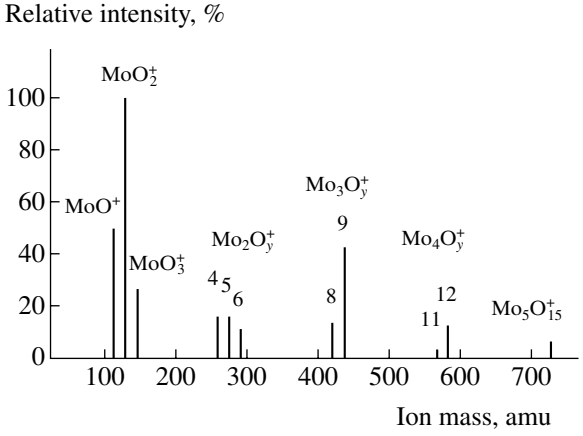


**Fig. 1.** Mass spectrum of positive molybdenum oxo ions obtained by $^{98}MoO_3$ evaporation from a Knudsen effusion source, 600 K.

The energy was calculated as the sum of the Coulomb interaction and the Born–Mayer repulsion

$$U_{ij} = \frac{q_i q_j}{r_{ij}} + A\exp\left[-\frac{r_{ij}}{\rho}\right]. \qquad (2)$$

Here, $r_{ij}$ is the interatomic distance for each pair of atoms; $q_i$ and $q_j$ are the formal atomic charges determined from the stoichiometry; $A$ and $\rho$ are varied parameters, which were chosen so that the bond lengths in a monomer and in the bulky molybdenum trioxide remained unchanged. The following values were used in the calculations: $A = 2256$ e$^2$/Å and $\rho = 0.181$ Å. In the calculations, it was assumed that the Mo–Mo bond was absent. A model of this kind was used for evaluating the geometry of the ions of cobalt and titanium oxides [13–15]. The results of the calculations demonstrated that oxygen-deficient and stoichiometric oxides can be structurally different, and this difference is responsible for differences in the reactivity.

Several low-energy isomers were found for each of the cluster oxo ions of molybdenum. Table 1 summarizes the optimum structures of all molybdenum oxides together with the calculated total energies of the molecules and the energies per cluster atom.

The $MoO_2^+$ and $MoO_3^+$ ions contained structurally and energetically equivalent oxygen atoms. Kretzshmar *et al.* [16] performed accurate quantum-chemical calculations of the structure and bond energies of the $MoO_3^+$ ion. They found that $MoO_3^+$ ($2A^2$) exhibits $C_{3v}$ symmetry and that all the oxygen atoms are equivalent (see structure **III**); that is, deviations from the cor-

**Table 1.** Bond energies in molybdenum oxides and oxo ions, ionization potentials, low-energy structures of molybdenum, and calculated energies per atom

| Oxide | Ionization potential, kcal/mol | Bond energy, kcal/mol | | | | | Structure | Cluster energy per atom, kcal/mol |
|---|---|---|---|---|---|---|---|---|
| | | tabulated | | calculated | | experimental $M^+$–O | | |
| | | M–O | M–$MoO_3$ | $M^+$–O | $M^+$–$MoO_3$ | | | |
| MoO | 173 | 120 | – | 98.5 | – | <151 [25]<br>118 ± 2 [31] |  | –80.1 |
| $MoO_2$ | 217 | 158 | – | 121 | – | >118 [25]<br><127 [32]<br>131 ± 5 [31] |  | –92.5 |
| $MoO_3$ | 277 | 143 | – | 83 | – | >85 <118 [25]<br><127 [32]<br>62 ± 7 [31] | 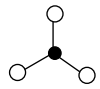 | –89.7 |
| $Mo_2O_4$ | – | – | – | – | – | – | 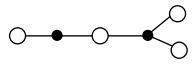 | –85.8 |
| $Mo_2O_5$ | 238 | – | – | – | – | – | 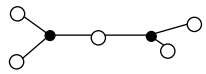 | –90.8 |
| $Mo_2O_6$ | 280 | 104 | 114 | 56 | 112 | <127 [32] | 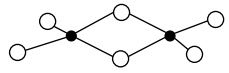 | –89.0 |
| $Mo_3O_8$ | 282 | – | – | – | – | – | 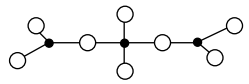 | –88.7 |
| $Mo_3O_9$ | 277 | 53 | 86 | 58 | 86 | <127 [32] | 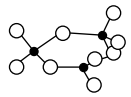 | –94.5 |
| $Mo_4O_{12}$ | 277 | – | 73 | – | 73 | – | 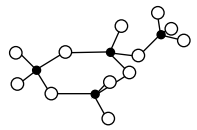 | –85.6 |
| $Mo_5O_{15}$ | 277 | – | 76 | – | 78 | – | 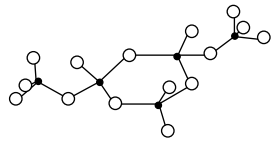 | –83.6 |

responding data for a neutral molecule of $MoO_3$ are small ($r_{Mo–O}$ = 1.70 Å; $C_{3v}$).

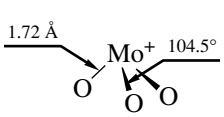


**III**

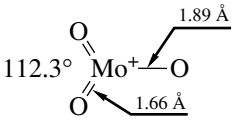


**IV**

Structure **IV** of $MoO_3^+$ ($2B_2$) exhibited an insignificantly higher energy (by 4 kcal/mol) than that of structure **III**. However, the symmetry reduced to $C_{2v}$, and the oxygen atoms became structurally and energetically nonequivalent; this was most clearly pronounced in the structure of dimers and trimers.

The structures of dimers and trimers (see Table 1) contain bridging and terminal oxygen atoms. The (bridging) oxygen atoms of the angular Mo–O–Mo groups are more strongly bound; the greatest electron density is concentrated at these atoms because of the strong inverse $d_\pi$–$P_\pi$ interaction. It is believed that these atoms are the localization centers of outer protons in heteropoly acids [17].

The $Mo_3O_9^+$ ion exhibits a cyclic structure, which is the most thermodynamically favorable. The $Mo_3O_9$ cyclic unit is retained in the structures of $Mo_4O_{12}^+$ and $Mo_5O_{15}^+$ ions.

## RESULTS AND DISCUSSION

A great body of experimental data on the activation of C–H and C–C bonds in hydrocarbons by transition metal ions has accumulated in the past two decades [18]. It is believed that the interaction of "naked" (i.e., not bound to ligands) metal ions occurs via the following main steps (Fig. 2):

(1) The formation of an amorphous encounter complex due to the interaction of the ion and the dipole induced in a neutral molecule. For a singly charged ion and $C_3$–$C_4$ hydrocarbons, the energy of this interaction is 10–15 kcal/mol. Usually, this energy is sufficient into overcome internal barriers and into insert the ion into the C–H or C–C bond of the hydrocarbon.

(2) The oxidative addition of the metal ion at the C–H (or C–C) bond of the hydrocarbon. In this case, the cleavage of the C–H (or C–C) bond and the formation of two new $M^+$–C and $M^+$–H bonds, where $M^+$ is the metal ion, takes place. Because only the occurrence of exothermic reactions in the gas phase can be observed using the ICR technique, the energy of the final products, as well as of all the intermediate compounds, should be lower than the energy of the initial reactants; that is, the sum of the energies of the resulting $M^+$–C and $M^+$–H bonds should be higher than the energy of the initial C–H (or C–C) bond of the hydrocarbon.

(3) The transfer of a β-hydrogen atom to the metal ion (β-shift) with the formation of a dihydride metal–alkene complex (H–$M^+$–(H)–R). The general tendency is that the β-hydrogen shift from a secondary carbon atom occurs more easily than that from a primary carbon atom. In the case of branched hydrocarbons, the transfer of a hydrocarbon fragment, for example, a $CH_3$ group, can also occur.

(4) The elimination of a hydrogen (or alkene) molecule and the formation of a final metal–alkene complex. Next, the metal ion can attack the following C–H or C–C bond leading to the formation of secondary reaction products. A comparison of the bond energies of metal ions with various ligands demonstrated that the $Cr^+$ ion forms weak binary metal–carbon and metal–hydrogen bonds; because of this, the step of insertion into the C–H bond (step (2)) is strongly endothermic. In the reactions of $Mo^+$ ions, it is likely that the step of addition at the C–H bond is almost thermally neutral (Fig. 2); the $W^+$ ion also reacts with butane to form dehydrogenation products [19, 20].

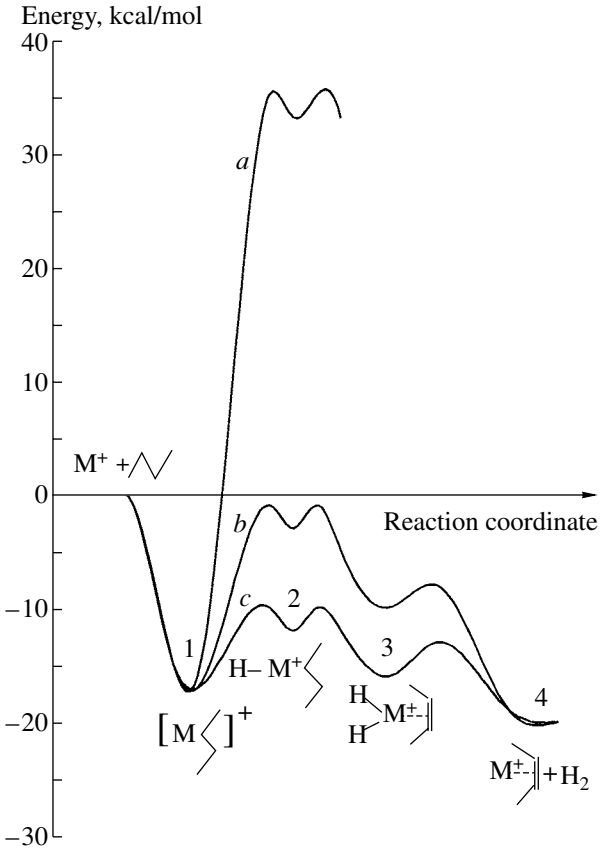


**Fig. 2.** Energy reaction diagram for the dehydrogenation of the *n*-butane molecule by (*a*) $Cr^+$, (*b*) $Mo^+$, and (*c*) $W^+$ ions.

The reactivity of the oxo ions of metals strongly depends on the bond energy $D^0(M^+–O)$. Thus, the reactivity of $FeO^+$ [21], $CrO^+$ [22], and $OsO^+$ [23] ions, which have a low (70–85 kcal/mol) bond energy with oxygen, increases when compared to naked metal ions because of the appearance of new reaction paths with the participation of the oxygen ligand (the formation of OH groups and the oxidation of hydrocarbons). However, the reactivity of the $VO^+$ ion, which has a very strong bond (134 kcal/mol) with the oxygen ligand, is lower than that of $V^+$ [24]. In this case, the oxygen ligand cannot participate in oxidation reactions; it only occupies a coordination site at the metal ion.

Direct evidence for the capacity of $Mo^+$ and $W^+$ ions for insertion into the C–H bonds of hydrocarbons followed by dehydrogenation was obtained with the use of tandem mass spectrometry and ICR mass spectrometry [19, 20].

Previously [20], it was found that $Mo^+$ ions react with cyclopropane to form dehydrogenation products.

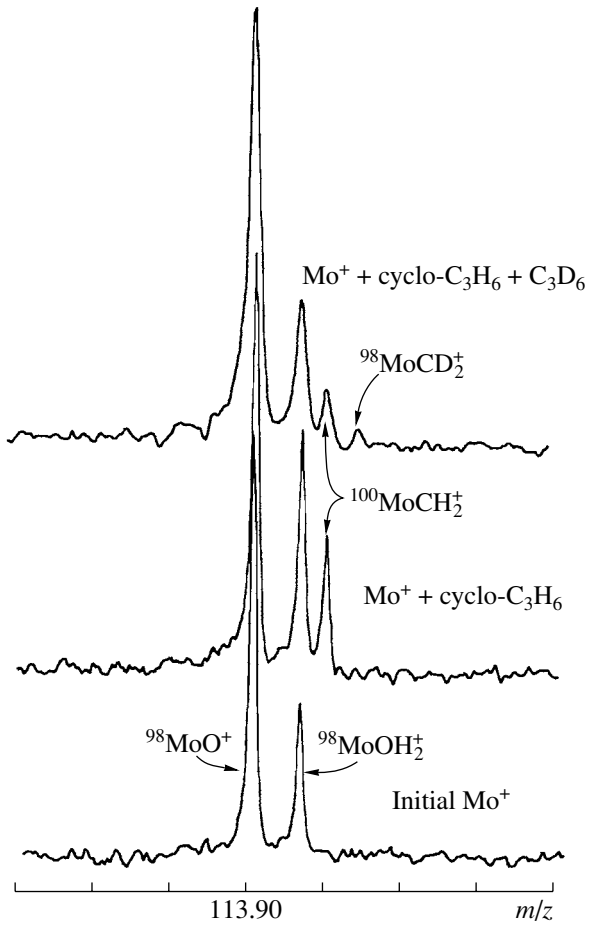


**Fig. 3.** High-resolution mass spectra of the reaction products of $Mo^+$ ions with cyclopropane and deuterated propylene ($C_3D_6$) molecules.

It was also found that the $Mo^+$ ion is primarily inserted into a C–C bond rather than a C–H bond. The C–H bond energy in the cyclopropane molecule is sufficiently high, equal to 106 kcal/mol, whereas the C–C bond is weaker (~54 kcal/mol) [11].

This study of the interaction of $Mo^+$ ions with a number of small alkanes and alkenes ($C_1$–$C_3$) demonstrated that the $MoCH_2^+$ metallocarbene was formed in small amounts (1–3% of the initial concentration of $Mo^+$) because of nonadiabatic electron-impact ionization and the generation of the molybdenum ion in an electronically excited state. The $MoCH_2^+$ ions were formed with a maximum yield (10–15% of the initial concentration of the metal cation) in the reaction with cyclopropane.

The high resolution of an ICR spectrometer provides an opportunity to distinguish the composition of complexes with close total ligand weights. With the use of accurate values of relative atomic weights (to the fourth and fifth decimal places), lines that correspond to complexes of different compositions can be identified unambiguously. Figure 3 demonstrates the fragments of high-resolution mass spectra recorded at $m/z = 114$.

This fragment exhibits two lines, which were attributed to $^{98}MoO^+$ and $^{96}MoOH_2^+$ ions. These ions are formed by the interaction of $Mo^+$ with background oxygen and water molecules. The complete removal of these impurities is a serious problem, and a small fraction of them is always present in the mass spectra. On the other hand, lines due to these ions are reference lines of sorts, which provide an opportunity to measure more accurately $m/z$ for organometallic ions formed in this region of the spectrum.

On the addition of cyclo-$C_3H_6$ ($P_{\text{cyclo-}C_3H_6} = 1 \times 10^{-7}$ mbar) to the vacuum system, the formation of $MoCH_2^+$ metallocarbene species was observed, and a corresponding line due to the $^{100}MoCH_2^+$ isotope appeared in the above mass range (Fig. 3). The addition of deuterated propylene ($P_{C_3D_6} = 1 \times 10^{-7}$ mbar) along with cyclopropane to the system resulted in a decrease in the line due to $^{100}MoCH_2^+$ and in the appearance of a new line with a greater $m/z$. The accurate measurement of the difference between $m/z$ of this and other lines makes it possible to identify unambiguously this line as that corresponding to the $^{98}MoCD_2^+$ ion. On the addition of only $C_3D_6$ to the system, this ion was not formed, and only the dehydrogenation products $MoC_3D_4^+$ were detected. Intermediates with the composition $MoCHD^+$ were also not detected; this circumstance (the absence of rapid H/D exchange) suggests that the exchange of $CH_2$ and $CD_2$ groups occurs in this reaction system. It is likely that the metathesis reaction occurs via the four-centered metal–cyclobutane intermediate **II**.

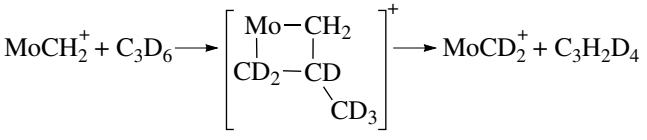


**II**

**Scheme 2.**

Evidently, the metathesis reaction is thermoneutral because the energies of cleaved and formed bonds are equal. It is likely that the occurrence of a particular step of this reaction under the conditions of ICR experiments is associated with the fact that the metallocarbene ion in an excited state is formed in the reaction with cyclopropane.

The interaction of $MoCH_2^+$ with deuterium ($P_{D_2}$ = $1 \times 10^{-5}$ mbar) did not result in the formation of the mixed products $MoCHD^+$ and $MoCD_2^+$.

Attempts to increase metallocarbene concentration in the gas phase by the interaction of the molybdenum ion with diazomethane were unsuccessful because of the degradation of the latter at the metal walls of the vacuum system.

Previously [25], the oxidation of $Mo^+$ and $W^+$ ions by various oxygen-containing oxidizing agents (NO, $O_2$, and $N_2O$) was studied. It was found that, with the use of $N_2O$ ($D^0(N_2–O)$ = 44 kcal/mol), the consecutive oxidation of metal cations to oxo ions occurred:

$$Mo^+ + N_2O \longrightarrow MoO^+ + N_2, \quad \text{(III)}$$

$$MoO^+ + N_2O \longrightarrow MoO_2^+ + N_2, \quad \text{(IV)}$$

$$MoO_2^+ + N_2O \longrightarrow MoO_3^+ + N_2. \quad \text{(V)}$$

This made it possible to estimate the bond energies of oxygen $D^0(MoO_n^+–O)$ ($n$ = 0–2) in the oxo ions of molybdenum: $D^0(Mo^+–O) > 151$ kcal/mol; $151 > D^0(MoO^+–O) > 118$ kcal/mol; $118 > D^0(MoO_2^+–O) >$ 85 kcal/mol.

The $Mo^+$ ion reacted with ethylene oxide ($D^0(C_2H_4–O)$ = 85 kcal/mol) to form sequentially molybdenum monoxide, dioxide, and trioxide cations and the $MoO_2CH_4^+$ ion (see Fig. 4):

$$Mo^+ + C_2H_4O \longrightarrow MoO^+ + C_2H_4, \quad \text{(VI)}$$

$$MoO^+ + C_2H_4O \longrightarrow MoO_2^+ + C_2H_4, \quad \text{(VII)}$$

$$MoO_2^+ + C_2H_4O \longrightarrow MoO_3^+ + C_2H_4, \quad \text{(VIII)}$$

$$MoO_2^+ + C_2H_4O \longrightarrow MoO_2CH_4^+ + CO. \quad \text{(IX)}$$

The $MoO_2CH_4^+$ ion resulted from a complex intramolecular rearrangement (Scheme 3).

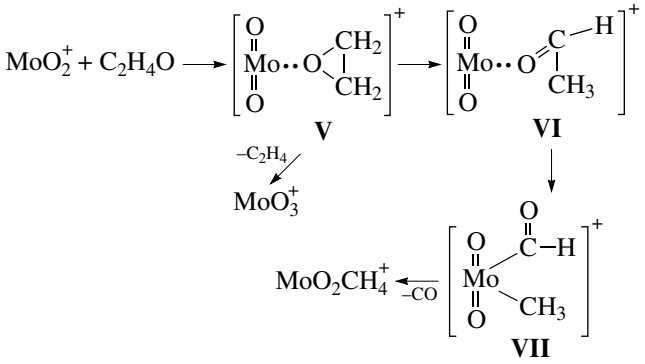


**Scheme 3.**

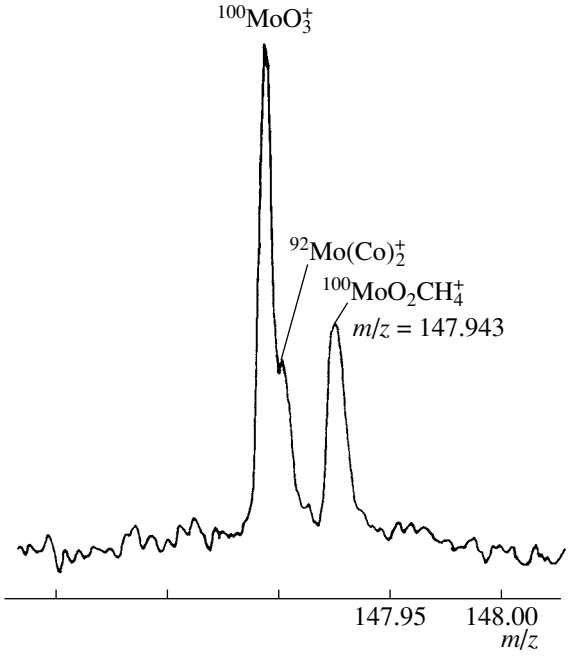


**Fig. 4.** High-resolution mass spectrum of the reaction products of $Mo^+$ ions with ethylene oxide.

The ethylene oxide molecule coordinated to the molybdenum ion (**V**) isomerized into acetaldehyde (**VI**) and was attacked by the metal ion at the C–C bond. The subsequent decarbonylation of intermediate **VII** resulted in the formation of the $MoO_2CH_4^+$ ion. This ion was isolated using the double resonance technique; then, it reacted with $D_2$ ($P_{D_2}$ = (1–2) × $10^{-5}$ mbar). It was experimentally found that consecutive H/D exchange rapidly occurred, and at least two hydrogen atoms were readily exchanged for deuterium. This fact suggests that the structure of the $MoO_2CH_4^+$ ion can be represented by intermediates **VIII** and **IX** (Scheme 4).

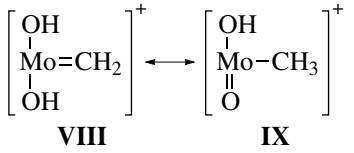


**Scheme 4.**

It is likely that H/D exchange can further occur because the isotopic label in the structure of **IX** can be redistributed to the organic fragment; however, this process is slower, and it cannot be detected using the ICR technique because of the high pressure of $D_2$ and diffusion losses of ions to the cell walls.

Consecutive H/D exchange also occurred in the reaction of the $MoO_2CH_4^+$ ion with deuterated propylene. Thus, the metathesis reaction was not detected.

Note that a great quantity of energy can be released in the course of oxidation (reactions (IV) and (V)) to

**Table 2.** Distribution of the products of $Mo_xO_y^+$ reactions with cyclopropane, %

| Ion | Product | | | | |
|---|---|---|---|---|---|
| | $Mo_xO_y(C_3H_4)^+$ | $Mo_xO_{y-1}(C_3H_4)^+$ | $Mo_xO_y(CH_2)^+$ | $Mo_xO_y(C_2H_4)^+$ | $Mo_xO_y(CH_4)^+$ |
| $Mo^+$ | 100 | – | – | – | – |
| $MoO^+$ | 100 | – | – | – | – |
| $MoO_2^+$ | – | 15 | 20 | 23 | 42 |
| $MoO_3^+$ | – | 100 | – | – | – |
| $Mo_2O_4^+$ | – | 36 | 64 | – | – |
| $Mo_2O_5^+$ | – | 34 | 34 | 16 | 16 |
| $Mo_2O_6^+$ | – | 100 | – | – | – |
| $Mo_3O_8^+$ | – | 32 | 15 | – | 53 |
| $Mo_3O_9^+$ | – | 100 | – | – | – |

result in the excitation of reaction products. Excited metal oxides can exhibit anomalously high reactivity. Thus, Kappes and Staley [26] found that the vanadium monoxide ion, obtained by the oxidation of a vanadium ion with $N_2O$, reacted with methane and hydrogen to abstract a hydrogen atom, whereas the $VO^+$ ion (prepared by the oxidation of $V^+$ with molecular oxygen) did not react with the above reagents. This phenomenon can be explained by the vibrational excitation of the $VO^+$ ion in the highly exothermic oxidation reaction of vanadium ions.

To decrease the effect of excited products, all the subsequent experiments were performed with the use of a Knudsen source. The ions formed by the electron-impact ionization of $^{98}MoO_3$ vapor were separated using the double resonance technique; these ions reacted with methane and cyclopropane.

The occurrence of oxygen ligands at molybdenum ions did not result in the appearance of the products of direct methane dehydrogenation; that is, reaction (X) did not occur. This can be explained by the fact that the formation of a carbene ($:CH_2$) from methane requires energy consumption (111 kcal/mol). This value can serve as an upper limit for the bond strength of $Mo_xO_y^+$ ions with carbene ($x = 1$–3; $y = 1$–9), $D^0(Mo_xO_y^+ – CH_2) <$ 111 kcal/mol.

$$Mo_xO_y^+ + CH_4 \not\longrightarrow Mo_xO_yCH_2^+ + H_2. \qquad (X)$$

The products of the oxidative dehydrogenation of methane (reaction (IX)) were detected only for ions with the $MoO_3$ stoichiometry ($Mo_2O_6$, $Mo_3O_9$). Taking into account the energy of abstraction of two hydrogen atoms from the $CH_4$ molecule [18], the energies of formation of the OH radical and the water molecule [18], and the exothermicity of reaction (XI), the lower limit of the bond energy $D^0(Mo_xO_{y-1}^+–CH_2)$ is estimated at 82 kcal/mol ($x = 1$–3; $y = 2, 5, 8$).

$$Mo_xO_{y-1}^+ + CH_4 \longrightarrow Mo_xO_yCH_2^+ + H_2O \qquad (XI)$$

Table 2 summarizes data on the distribution of reaction products of molybdenum oxide ions with cyclopropane. These data indicate that the addition of an oxygen ligand had no effect on the reactivity of the molybdenum ion. The reaction of dehydrogenation, which occurred in the case of the $Mo^+$ ion, was also observed for $MoO^+$:

$$MoO^+ + cyclo\text{-}C_3H_6 \longrightarrow MoO(C_3H_4)^+ + H_2. \qquad (XII)$$

Here, the oxygen ligand was not involved in the reaction. Cassady and McElvany [27], who studied the interaction of $MoO^+$ with various hydrocarbons, arrived at a similar conclusion. Based on this information, the sufficiently strong $Mo^+$–O bond ($D^0 > 118$ kcal/mol) should not be cleaved in the course of the reaction.

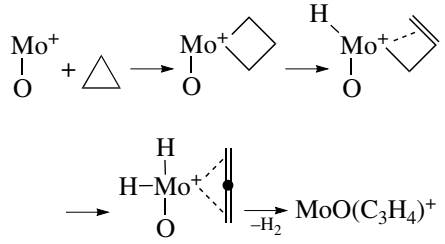

**Scheme 5.**

A hypothetical mechanism of the interaction of $MoO^+$ with cyclopropane includes the initial insertion of $Mo^+$ into the C–C bond, the formation of a metallo-

cycle, and a two-step transfer of a β-hydrogen atom to the metal ion (Scheme 5). The subsequent elimination of $H_2$ results in the formation of the $MoO^+$–allene complex. This mechanism is identical to the mechanism proposed for $Mo^+$ [20, 27]. The insertion of $Mo^+$ into the C–H bond of cyclopropane can result in the same reaction products as insertion into the C–C bond. However, as mentioned above, insertion into the C–C bond is thermodynamically preferable.

The reactivity of $MoO_2^+$ in reactions with cyclopropane is dramatically different from the reactivity of $Mo^+$ and $MoO^+$. Data given in Table 2 suggest that $MoO_2^+$ readily eliminates an oxygen ligand to form $MoOC_3H_4^+$ and water.

$$MoO_2^+ + \text{cyclo-}C_3H_6 \longrightarrow MoO(C_3H_4)^+ + H_2O. \quad \text{(XIII)}$$

However, the oxidative dehydrogenation of cyclopropane is not the main reaction path of $MoO_2^+$. Insertion into the C–C bond of cyclopropane is preferable, which results in the degradation of the carbon skeleton and in the formation of metal–carbene species:

$$MoO_2^+ + \text{cyclo-}C_3H_6 \longrightarrow MoO_2CH_2^+ + C_2H_4, \quad \text{(XIV)}$$

$$MoO_2^+ + \text{cyclo-}C_3H_6 \longrightarrow MoO_2C_2H_4^+ + CH_2, \quad \text{(XV)}$$

$$MoO_2^+ + \text{cyclo-}C_3H_6 \longrightarrow MoO_2CH_4^+ + C_2H_2. \quad \text{(XVI)}$$

Scheme 6 illustrates a hypothetical mechanism of the formation of a metal–carbene species. An attack of $Mo^+$ on a bond in the metallocycle results in the formation of intermediate **X**, which can eliminate either ethylene (reaction (XIV)) or $CH_2$ (reaction (XV)). However, the conversion of intermediate **X** into intermediate **XI** is a [2 + 2]-addition reaction, which is forbidden by Woodward–Hoffmann symmetry rules. A theoretical consideration of systems of this kind demonstrated that this conversion becomes possible when the bond mainly exhibits a δ character [28]. Thus, the difference in the reactivity of $MoO^+$ and $MoO_2^+$ can be explained by the fact that $MoO^+$ largely exhibits an *s* character of the bond as compared with $MoO_2^+$. Formation of the reaction product $MoO_2CH_4^+$ occurs in the subsequent dehydrogenation of intermediate **X**. It is most likely that acetylene is the neutral product of this reaction.

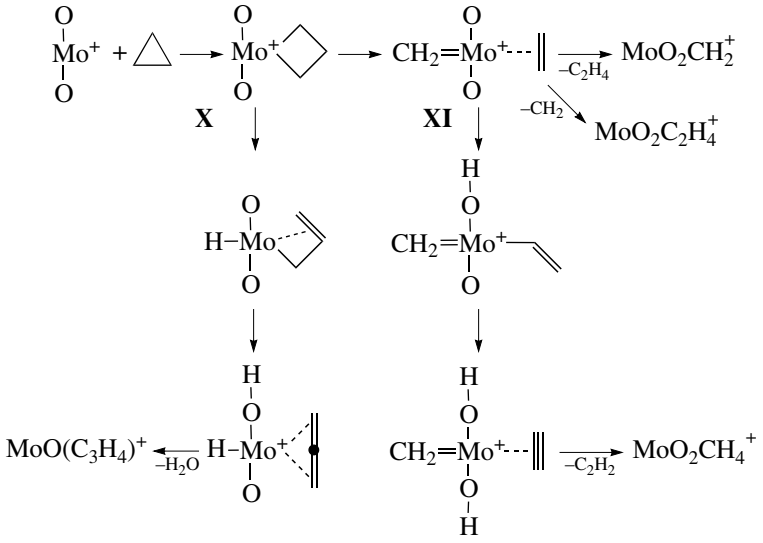


**Scheme 6.**

Scheme 6 also demonstrates the mechanism of the oxidative dehydrogenation of cyclopropane. In general, it is identical to the reaction mechanisms of $Mo^+$ and $MoO^+$ with cyclo-$C_3H_6$. As the number of free coordination sites at the molybdenum ion decreases, the attachment of a hydrogen atom to the oxygen ligand rather than the metal ion becomes more preferable. Next, cleavage of the strong $OMo^+$–O bond is compensated by energy released in the formation of the water molecule.

$Mo^+$ possesses five *d* electrons, which make it possible to form five covalent bonds. Molybdenum oxo structures contain bridging and terminal oxygen atoms, that is, Mo–O–Mo and –Mo=O groups, even in aqueous solutions. However, the formation of ordinary $Mo^+$–O bonds, which are nontypical of the aqua forms of molybdenum oxo ions, should be assumed in some steps to explain the formation of the reaction products in the gas phase.

Based on the above consideration, one oxygen ligand in the $MoO_3^+$ ion should formally possess an ordinary bond with the molybdenum ion. That is, $MoO_3^+$ should be a radical ion, which exhibits an enhanced reactivity. This may explain the observed increase in the rate of $MoO_3^+$ reaction with cyclopropane.

Because all the coordination sites at $Mo^+$ in $MoO_3^+$ are occupied, reactions should occur with the insertion of the $Mo^+$–O fragment into the C–C bond of cyclopropane. The initial loss of an oxygen ligand is also possible; this is highly probable because the third oxygen ligand is bound less strongly than the others (Table 1) [25]. The absence of free coordination sites prevents the formation of carbene species (Scheme 7).

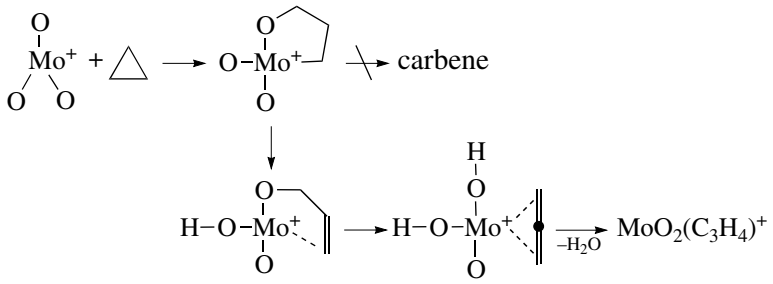


**Scheme 7.**

The oxo ions of molybdenum containing two and three metal atoms retained the same reaction paths as in the case of monomers, namely, the dehydrogenation of cyclopropane and the formation of carbene particles (Table 2). An increase in the particle size had no effect on the reactivity of molybdenum oxo ions with cyclopropane.

For $Mo_2O_4^+$, the main reaction was the formation of $Mo_2O_4CH_2^+$, which occurred with the elimination of an ethylene molecule. The formation of other carbene species was not detected.

The $Mo_2O_5^+$ and $Mo_3O_8^+$ ions, which are structurally equivalent to $MoO_2^+$, enter into the same reactions as $MoO_2^+$. Some differences were observed in the distribution of reaction products. In the case of $Mo_3O_8^+$, the product $Mo_3O_8(C_2H_4)^+$ was not formed. In general, it is believed that the reaction occurs via the same mechanism as with $MoO_2^+$. Previously, it was found that dimers and trimers are stable under the reaction conditions; that is, the fragmentation of these ions does not occur in the interaction with cyclopropane.

The coordinatively unsaturated molybdenum oxo ions $Mo_2O_6^+$ and $Mo_3O_9^+$, as well as their analog $MoO_3^+$, only enter into the reaction of cyclopropane dehydrogenation. The abstraction of an oxygen ligand from these oxo ions can occur more readily because the $Mo^+$–O bond becomes weaker as the ionic size increases.

Thus, the experimental results indicate that the dehydrogenation of cyclopropane can occur at one molybdenum atom surrounded by oxygen ligands. Only coordinatively unsaturated molybdenum atoms are reactive in the formation of carbene species. The presence of a neighboring molybdenum atom can result in a decrease in the $Mo^+$–O bond energy on the one hand and in steric hindrances on the other hand.

According to Vikulov *et al.* [29], the $Mo{=}CH_2$ bond energy in complex **XII** is equal to 104 kcal/mol; that is, it is consistent with the experimental data obtained by the ICR technique.

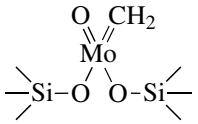

**XII**

Note that organometallic ions detected in this work were considered previously as intermediate species in order to explain the metathesis reactions of olefins and the photoactivated adsorption of alkanes on supported $MoO_3/SiO_2$ systems [29, 30].

## ACKNOWLEDGMENTS

This work was supported by the International Science Foundation (grant nos. RBG 000 and RBG 300).

I am grateful to A.V. Kikhtenko and E.F. Fialko for their assistance in performing the experiments and for helpful discussions.

## REFERENCES

1. Banks, R.L. and Bailey, G.C., *Ind. Eng. Chem. (Prog. Res. Dev.)*, 1964, vol. 3, p. 170.

2. Irvin, K.J., *Olefin Metathesis*, New York: Academic, 1983, p. 339.
3. Krylov, O.V. and Matyshak, V.A., *Promezhutochnye soedineniya v geterogennom katalize* (Intermediate Species in Heterogeneous Catalysis), Moscow: Nauka, 1996, p. 50.
4. Shelimov, B.N., Pershin, A.N., and Kazansky, V.B., *J. Catal.*, 1980, vol. 64, p. 426.
5. Nefedov, O.M., Ioffe, A.I., and Menchikov, L.G., *Khimiya karbenov* (The Chemistry of Carbenes), Moscow: Khimiya, 1990, p. 236.
6. Parent, D.C. and Anderson, S.L., *Chem. Rev.*, 1992, vol. 92, no. 3, p. 1541.
7. Smith, D. and Adams, N.G., *Gas-Phase Ion Chemistry*, Bowers, M., Ed., New York: Academic, 1979, vol. 1.
8. Cassady, C.L., Weil, D.A., and McElvany, S.W., *J. Chem. Phys.*, 1992, vol. 96, p. 691.
9. Maleknia, S., Brodbelt, J., and Pope, K., *J. Am. Chem. Soc., Mass. Spectr.*, 1991, vol. 2, p. 212.
10. Allemann, M., Kellerhals, Hp., and Wanczek, K.-P., *Chem. Phys. Lett.*, 1980, vol. 75, p. 328.
11. *Energiya razryva khimicheskikh svyazei. Potentsialy ionizatsii i srodstvo k elektronu* (Chemical Bond Energies: Ionization Potentials and Electron Affinities), Kondrat'ev, V.N., Ed., Moscow: Nauka, 1974.
12. Goncharov, V.B. and Fialko, E.F., *Zh. Strukt. Khim.*, 2002, vol. 43, no. 5, p. 839.
13. Freas, R.B., Dunlap, B.I., Waite, B.A., and Campana, J.E., *J. Chem. Phys.*, 1987, vol. 86, no. 3, p. 1276.
14. Freas, R.B. and Campana, J.E., *J. Am. Chem. Soc.*, 1986, vol. 108, no. 11, p. 4659.
15. Yu, W. and Freas, R.B., *J. Am. Chem. Soc.*, 1990, vol. 112, no. 21, p. 7126.
16. Kretzshmar, I., Fiedler, A., Harvey, J., Schroder, D., and Schwartz, H., *J. Phys. Chem.*, 1990, vol. 101, no. 35, p. 6252.
17. Kazanskii, L.P., *Dokl. Akad. Nauk SSSR*, 1973, vol. 209, p. 141.
18. Eller, K. and Schwartz, H., *Chem. Rev.*, 1991, vol. 91, p. 1121.
19. Kikhtenko, A.V., Goncharov, V.B., Momot, K.I., and Zamaraev, K.I., *Organometallics*, 1994, vol. 13, p. 2536.
20. Schilling, J.B. and Beauchamp, J.L., *Organometallics*, 1988, vol. 7, p. 194.
21. Jackson, T.C., Jacobson, D.B., and Freiser, B.S., *J. Am. Chem. Soc.*, 1984, vol. 106, p. 1252.
22. Kang, H. and Beauchamp, J.L., *J. Am. Chem. Soc.*, 1986, vol. 108, no. 19, p. 5663.
23. Irikura, K.K. and Beauchamp, J.L., *J. Am. Chem. Soc.*, 1989, vol. 111, no. 1, p. 75.
24. Jackson, T.C., Carlin, T.J., and Freiser, B.S., *J. Am. Chem. Soc.*, 1986, vol. 108, no. 1, p. 75.
25. Kikhtenko, A.V., Goncharov, V.B., and Zamaraev, K.I., *Catal. Lett.*, 1993, vol. 21, no. 2, p. 353.
26. Kappes, M.M. and Staley, R.H., *J. Phys. Chem.*, 1981, vol. 85, no. 3, p. 942.
27. Cassady, C.J. and McElvany, S.W., *Organometallics*, 1992, vol. 11, no. 7, p. 2367.
28. Steigerwald, M.L. and Goddard III, W.A., *J. Am. Chem. Soc.*, 1984, vol. 106, no. 2, p. 308.
29. Vikulov, K.A., Elev, I.V., Shelimov, B.N., and Kazansky, V.B., *J. Mol. Catal.*, 1989, vol. 55, no. 1/3, p. 126.
30. Subbotina, I.R., Shelimov, B.N., and Kazanskii, V.B., *Kinet. Katal.*, 1997, vol. 38, no. 5, p. 742.
31. Kretzshmar, I., Fiedler, A., Harvey, J., *et al.*, *J. Phys. Chem.*, 1990, vol. 101, no. 35, p. 6252.
32. Fialko, E.F., *Cand. Sci. (Chem.) Dissertation*, Novosibirsk, 1998.